© 2020. Published by The Company of Biologists Ltd | Journal of Experimental Biology (2020) 223, jeb230375. doi:10.1242/jeb.230375

RESEARCH ARTICLE

Morphological colour adaptation during development in fish: involvement of growth hormone receptor 1

Tomás Horacio Delgadin[1,2], Diana Carolina Castañeda-Cortés[3], Clara Sacks[2], Andrés Breccia[2], Juan Ignacio Fernandino[3] and Paula Gabriela Vissio[1,2,*]

ABSTRACT

Morphological background adaptation is both an endocrine and a nervous response, involving changes in the amount of chromatophores and pigment concentration. However, whether this adaptation takes place at early developmental stages is largely unknown. Somatolactin (Sl) is a pituitary hormone present in fish, which has been associated to skin pigmentation. Moreover, growth hormone receptor type 1 (Ghr1) has been suggested to be the Sl receptor and was associated with background adaptation in adults. In this context, the aim of this work was to evaluate the ontogeny of morphological adaptation to background and the participation of *ghr1* in this process. We found in larval stages of the cichlid *Cichlasoma dimerus* that the number of head melanophores and pituitary cells immunoreactive to Sl was increased in individuals reared with black backgrounds compared with that in fish grown in white tanks. In larval stages of the medaka *Oryzias latipes*, a similar response was observed, which was altered by *ghr1* biallelic mutations using CRISPR/Cas9. Interestingly, melanophore and leucophore numbers were highly associated. Furthermore, we found that somatic growth was reduced in *ghr1* biallelic mutant *O. latipes*, establishing the dual function of this growth hormone receptor. Taken together, these results show that morphological background adaptation is present at early stages during development and that is dependent upon *ghr1* during this period.

KEY WORDS: Medaka, *ghr1*, *ghr2*, CRISPR/Cas9, Chromatophores, Background adaptation

INTRODUCTION

Skin pigmentation of vertebrates is mainly due to the presence of neural crest-derived cells termed chromatophores, which contain either light-absorbing or light-reflecting pigments in specialized intracellular structures called chromatosomes (Fujii, 1993). The pattern of pigmentation as well as the body colour the animal displays during its life are highly variable in vertebrates, constituting a good example of phenotypic plasticity (Sköld et al., 2016). Moreover, these features can change as a result of developmental constraints at embryo/larvae, larvae/juvenile or juvenile/adult transitions, or as a response to biotic or abiotic environmental cues such as nutrition, UV incidence, surrounding luminosity and social interactions (Leclercq et al., 2010). This process, termed morphological colour change, occurs during long periods of time and implies variations of chromatophore number or density and/or modifications in the chromatophore structure, such as cell size or pigment content (Leclercq et al., 2010). Another related process animals can display is physiological colour change, which occurs over short periods of time as an immediate response to environment changes by aggregating or dispersing pigment-containing vesicles (i.e. chromatosomes) inside the cell (Fujii, 1993). Both morphological and physiological colour changes are processes driven by endocrine and nervous systems.

Background adaptation, an example of physiological colour change, is widely observed in animals and refers to the organism's ability to change its body colour and/or its pattern of pigmentation as a consequence of changes in surrounding luminosity, such as dark or bright backgrounds. Interestingly, if background adaptation in adult fishes takes place over long periods of time, the physiological colour adaptation can be followed by a morphological one (Leclercq et al., 2010; Sköld et al., 2016; Sugimoto, 2002). In this sense, most long-term background adaptation studies have analysed melanophores, a type of chromatophore with a stellate shape containing a black/brown pigment called melanin (Fujii, 1993; Leclercq et al., 2010; Sugimoto, 2002). However, it would be interestingly to analyse how chromatophores other than melanophores behave after long-term background adaptation, particularly xanthophores, which are a light-absorbing chromatophore frequently found on fishes, smaller in size than melanophores and containing a yellow/orange pigment (Aspengren et al., 2008; Fujii, 1993), and leucophores, uncommon light-reflective chromatophores characterized by a white appearance. At the same time, the amount of chromatophores in the skin at a given time results from the balance between chromatophore production by differentiation and proliferation of stem cell and removal by apoptosis (Sugimoto et al., 2000; Sugimoto, 2002). Finally, as far as we know, it is not clear whether the morphological background adaptation process that is observed in adults could take place during early fish developmental stages.

Somatolactin (Sl) is a fish pituitary hormone that, along with growth hormone (Gh) and prolactin (Prl), forms a family of pituitary hormones, which are similar in structure, function and gene organization (Kawauchi and Sower, 2006). Several studies suggested a role of this hormone in a number of processes such as reproduction, stress responses, Ca^{2+} homeostasis, acid–base balance, growth, metabolism, immune responses and skin pigmentation (Benedet et al., 2008; Cánepa et al., 2006, 2012; Johnson et al., 1997; Kakisawa et al., 1995; Kaneko and Hirano, 1993; Laiz-Carrión et al., 2009; Mousa and Mousa, 2000; Planas et al., 1992; Uchida et al., 2009; Vargas-Chacoff et al., 2009; Vissio et al., 2002; Zhu et al., 1999). Additionally, it has been proposed that Sl is

[1]Universidad de Buenos Aires, Facultad de Ciencias Exactas y Naturales, Departamento de Biodiversidad y Biología Experimental, Buenos Aires C1428EGA, Argentina. [2]CONICET – Universidad de Buenos Aires, Instituto de Biodiversidad y Biología Experimental y Aplicada (IBBEA), Buenos Aires C1428EGA, Argentina. [3]Laboratorio de Biología del Desarrollo, Instituto Tecnológico de Chascomús (CONICET-UNSAM), Chascomús B7130IWA, Argentina.

*Author for correspondence (pvissio@gmail.com)

C.S., 0000-0002-2380-0049; A.B., 0000-0003-4902-1024; J.I.F., 0000-0003-1754-2802; P.G.V., 0000-0002-0240-9534

Received 2 June 2020; Accepted 22 October 2020

Journal of Experimental Biology (2020) 223, jeb230375. doi:10.1242/jeb.230375

involved in the generation of chromatophores and the regulation of pigment movements inside them (Cánepa et al., 2006; Fukamachi et al., 2004; Zhu et al., 1999). In red drum (*Sciaenops ocellatus*) and *Cichlasoma dimerus*, Sl was increased in the pituitary of adult fish adapted to dark backgrounds (Cánepa et al., 2006; Zhu et al., 1999), and in red drum this was concomitant with an increase in plasma S protein concentration (Zhu et al., 1999). Moreover, the mRNA of the putative Sl receptor has been localized in the epidermis and dermis cells from fish scales and has shown changes in transcript levels associated with changes in melanophore number (Cánepa et al., 2012). What is more, in a medaka Sl mutant (*ci* strain), defects in chromatophore proliferation and morphogenesis were observed (Fukamachi et al., 2004), and the transgenic over-expression of Sl in the *ci* genome rescued the wild phenotype (Fukamachi et al., 2009). Nevertheless, the evidence accumulated over the years has not completely unravelled the identity of the Sl receptor (Slr) in fish. Early studies carried out in salmonids have concluded that Gh receptor type 1 (Ghr1) is actually the Slr (Fukada et al., 2005) and Gh receptor type 2 (Ghr2) is the Gh receptor (Fukada et al., 2004). Although studies in other fish species give support for this hypothesis (Cánepa et al., 2012; Fukamachi and Meyer, 2007), recent research carried out in zebrafish has concluded that Sl is not a ligand for Ghr1; moreover, Gh is a ligand for both Ghr1 and Ghr2 (Chen et al., 2011). Thus, additional work is needed to explore the role of Sl and Ghr1 in the background adaptation process and in somatic growth in fish.

In this study, we provide evidence for the role of Sl and Ghr1 in the regulation of background adaptation during the early stages of development in two fish species, *Cichlasoma dimerus* (Heckel 1840) and medaka *Oryzias latipes* (Temminck and Schlegel 1846). Additionally, as *ghr1* and *ghr2* are paralogues, we demonstrate that *ghr1*, in addition to presenting a role in background adaptation, also has a role in somatic growth.

MATERIALS AND METHODS

Animals

Background adaptation: *C. dimerus*

Eggs from four independent *C. dimerus* spawnings were each divided into two groups and randomly placed into 2 l white or black tanks immediately after egg fertilization (Fig. 1A). Larvae were fed with newly hatched nauplii of *Artemia* sp. when reaching the free-swimming stage (5–6 days post-hatching, dph). After 12 dph, they were fed with ground commercial pellets (Kilomax Iniciador, 703; Mixes del sur, Florida, Buenos Aires, Argentina) of increasing size and proportion until 18 dph, when commercial food completely replaced *Artemia* sp. At 10, 15, 21 and 30 dph, three larvae from each background were withdrawn, anaesthetized on ice and submerged in 20 µg ml^{-1} dopamine solution to induce melanophore aggregation, placed at 0°C to reduce movements and observed under an optical magnifier. This protocol was repeated four times. All melanophores from the dorsal region of the head were

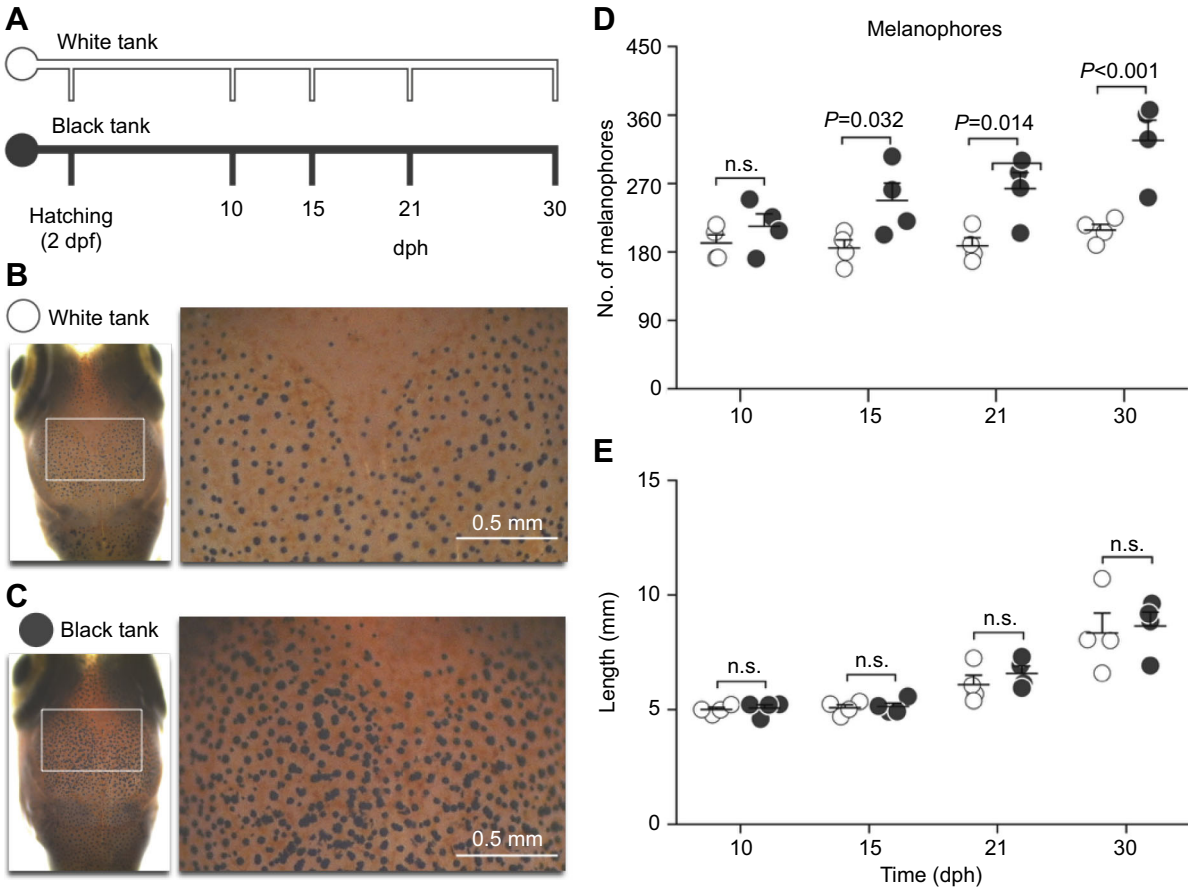

Fig. 1. Background adaptation of *Cichlasoma dimerus*. (A) Schematic representation of the experimental design; embryos were exposed from the day of fertilization until 30 days post-hatching (dph) to white or black tank environments. Hatching occurred at 2 days post-fertilization (dpf). Samples were collected at 10, 15, 21 and 30 dph. (B,C) White (B) and black (C) tank larvae at 30 dph. (D,E) Number of melanophores in the head (D) and standard length (E) of individuals reared in white (white circles) and black (black circles) tanks at different time points. Bars in D and E represent the mean value of four experimental replications, and each point the mean value of three larvae.

Journal of Experimental Biology (2020) 223, jeb230375. doi:10.1242/jeb.230375

manually counted from each larva. Total length was measured at each time point using ImageJ® (Bethesda, MD, USA) software after appropriate calibration. Additionally, at least two larvae from each background and spawning were placed at 0°C and then fixed in Bouin's solution for further histological analysis. All experiments comply with the approval of Comisión Institucional para el Cuidado y Uso de Animales de Laboratorio, Facultad de Ciencias Exactas y Naturales, Buenos Aires, Argentina (protocol number 95).

Background adaptation: *O. latipes*

Oryzias latipes eggs were taken from two to three spawnings of different male and female pairs for each time point and randomly assigned to black or white backgrounds, reared in a Petri dish until hatching and then transferred to tanks of the same background till sampling at 9, 12 and 16 dph (Fig. 3A). To measure dorsal head melanophore and xanthophore number and total length, the method previously described for *C. dimerus* was employed. The strain hi-medaka (ID: MT835) was supplied from the National BioResource Project (NBRP) Medaka (www.shigen.nig.ac.jp/medaka/). All medaka fish were maintained and fed following standard protocols for medaka (Kinoshita et al., 2012). Medaka fish were handled in accordance with the Universities Federation for Animal Welfare Handbook on the Care and Management of Laboratory Animals (www.ufaw.org.uk) and internal institutional regulations.

Immunohistochemistry assays

Larvae from *C. dimerus* and *O. latipes* sampled at 16 and 30 dph were fixed in Bouin's solution for 12 h in darkness at 4°C, dehydrated in an increasing alcohol/water graded solution, submerged in xylene for 5 min and then embedded in Paraplast® (Leica Biosystems, Germany). Transverse sections (7 µm) at the pituitary level were xylene treated twice for 35 min and then rehydrated in a graded alcohol series, ending in phosphate-buffered saline (PBS, pH 7.4). All sections were incubated for 5 min in 0.3% (v/v) H_2O_2 to block endogenous peroxidase. After three washes for 5 min in PBS, slices were blocked with 5% non-fat dried milk in PBS for 1 h and then incubated overnight at 4°C with rabbit anti-*Sparus aurata* Sl antiserum (1:1500, kindly donated by Dr Astola, University of Cadiz, Spain) (Astola et al., 1996) and anti-*Odontesthes bonariensis* Gh antiserum (1:3000, kindly donated by Dra Silvia Arranz, FCByF-UNR, Acuario del río Paraná, Argentina) (Sciara et al., 2006). Afterward, slices were washed three times in PBS for 5 min and incubated with biotinylated anti-rabbit IgG (1:500 in PBS, Sigma-Aldrich, St Louis, MO, USA) at room temperature (RT) for 1 h. Following three PBS washes, the sections were incubated with IgG peroxidase-conjugated streptavidin (dilution 1:500 in PBS; Invitrogen, Carlsbad, CA, USA) at RT for 1 h. The final step was accomplished by treating sections with 0.3% (w/v) 3,3-diaminobenzidine in Tris buffer (pH 7.6) and 0.02% (v/v) H_2O_2. Then, sections were subjected to a slight counterstaining with haematoxylin followed by a rapid dehydration step in graded alcohol to xylene and mounted in DPX. Slices were observed with a

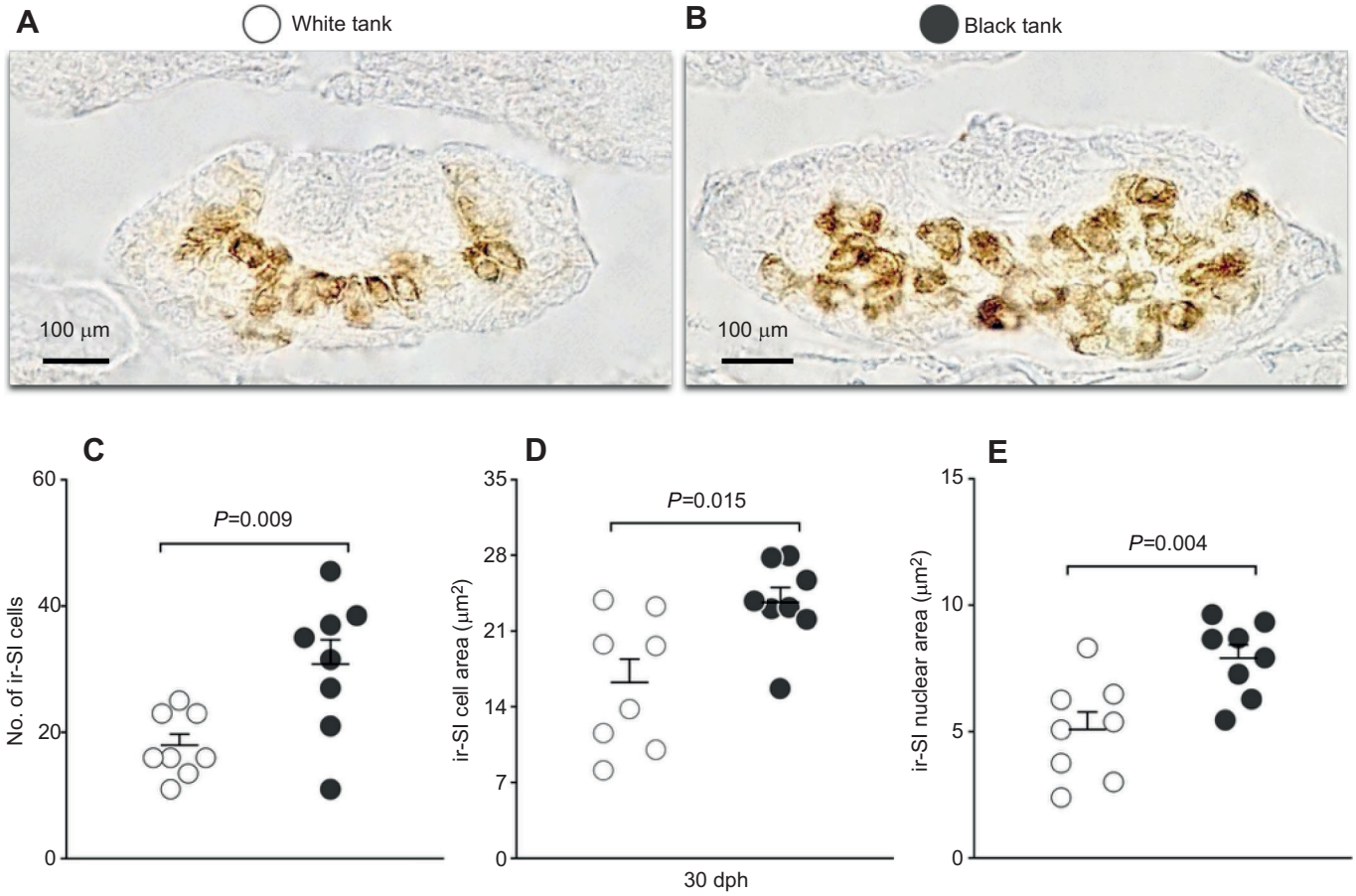

Fig. 2. Somatolactin response to background adaptation of *C. dimerus*. (A,B) Transverse sections of the pituitary gland from individuals exposed to white (A) and black (B) tank environments from the first day of fertilization until 30 dph, showing cells that are immunoreactive (ir) for somatolactin (Sl). (C–E) Number of ir-Sl cells (C), ir-Sl cell area (D) and ir-Sl nuclear area (E) of individuals reared in a white tank (white circles) or a black tank (black circles) at 30 dph. Sample size for each treatment, *n*=8.

Journal of Experimental Biology (2020) 223, jeb230375. doi:10.1242/jeb.230375

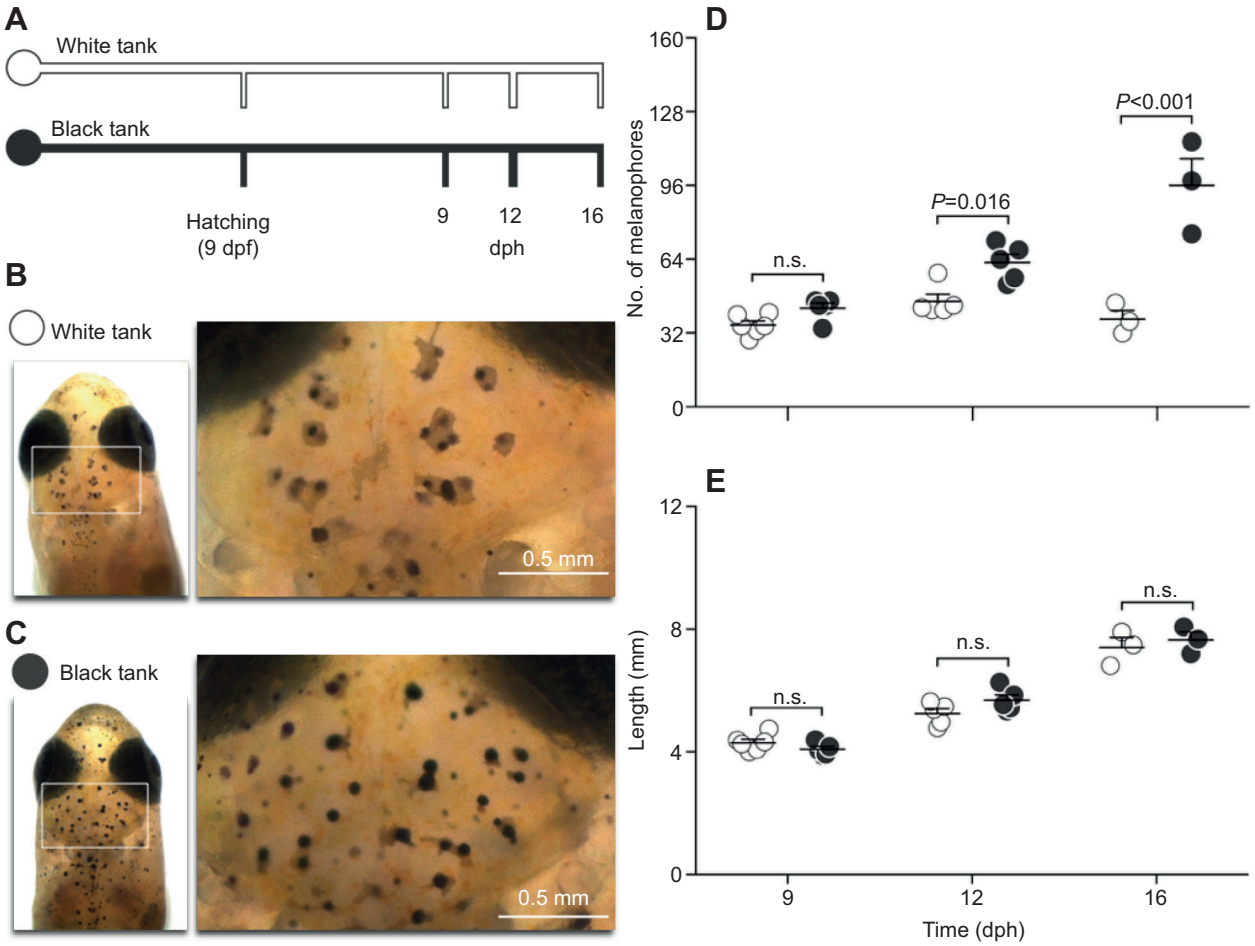

Fig. 3. Background adaptation of *Oryzias latipes*. (A) Schematic representation of the experimental design; embryos exposed were exposed from the day of fertilization until 16 dph to white or black tank environments. Hatching occurred at 9 dpf. Samples were collected at 9, 12 and 16 dph. (B,C) White (B) and black (C) tank larvae at 16 dph. (D) Number of melanophores in the head (D) and standard length (E) of individuals from white (white circles) and black (black circles) tanks at 9 dph (white n=6, black n=5), 12 dph (white n=5, black n=5) and 16 dph (white n=3, black n=3).

Microphot FX microscope (Nikon, Tokyo, Japan) and photographed if immunoreactive (ir)-Sl cells were present. Antibody specificity was analysed previously (Pandolfi et al., 2001). Counting of ir-cells for Gh and Sl was carried out for the slice with the highest number of ir-cells for a given pituitary gland.

Biallelic mutations of *ghr1* in *O. latipes* using CRISPR/Cas9

To analyse the participation of *ghr1* in the background adaptation, we performed a biallelic mutation using CRISPR/Cas9 following the protocol described previously (Ansai and Kinoshita, 2014; Castañeda Cortés et al., 2019). Briefly, target sites were designed using the CCTop - CRISPR/Cas9 target online predictor (crispr.cos.uni-heidelberg.de/index.html; Stemmer et al., 2015), which identified sequence 5′GG-(N18)-NGG3′ in exon 2 of *grh1* (AATGTGTATCAAGGGACCTGG; Fig. 4A). Then, for single guide RNA (sgRNA) synthesis, the annealed oligonucleotides were subcloned into the sgRNA expression vector pDR274 (Addgene #42250) (Hwang et al., 2013) and transcription was carried out using the MEGAshortscript T7 Transcription Kit (Thermo Fisher Scientific, Waltham, MA, USA). Additionally, the capped *cas9* RNA was transcribed from pCS2-nCas9n plasmid (Addgene #47929) and synthesized by mMESSAGE mMACHINE SP6 kit (Life Technologies, Carlsbad, CA, USA). The synthesized sgRNAs and *cas9* were purified using an RNeasy Mini kit (Qiagen, Hilden, Germany). These RNA sequences were diluted to 50 and 200 ng μl^{-1}, respectively.

Potential off-target sites in the medaka genome for each sgRNA were searched using the CCTop - CRISPR/Cas9 target online predictor (crispr.cos.uni-heidelberg.de/index.html; Stemmer et al., 2015). Only one potential off-target site was identified, in chromosome 13 (ENSORLG00000003362) and analysed by heteroduplex mobility assay (HMA) (Castañeda Cortés et al., 2019) using the primers: F 5′AGCTGTGTCAGCCTGTGAAA3′ and R 5′TGAGCGGGGAAAAACATTAC3′. Electrophoresis was performed (12% acrylamide gel; Ota et al., 2013) and the gel was stained with ethidium bromide for 15 min before examination.

Microinjection into *O. latipes* embryos and experimental design for background adaptation

Microinjection was performed into fertilized *O. latipes* eggs before the first cleavage as described previously (Kinoshita et al., 2000), using a Nanoject II Auto-Nanoliter Injector (Drummond Scientific, Broomall, PA, USA) coupled to a stereomicroscope (Olympus, Shinjuku, Tokyo, Japan). Embryos injected with only *cas9* were used as controls and randomly assigned to black or white backgrounds. For the CRISPR/Cas9 system, 4.6 nl of an RNA mixture of 25 ng μl^{-1} *sgRNA* and 100 ng μl^{-1} *cas9* was co-injected into the embryos.

Journal of Experimental Biology (2020) 223, jeb230375. doi:10.1242/jeb.230375

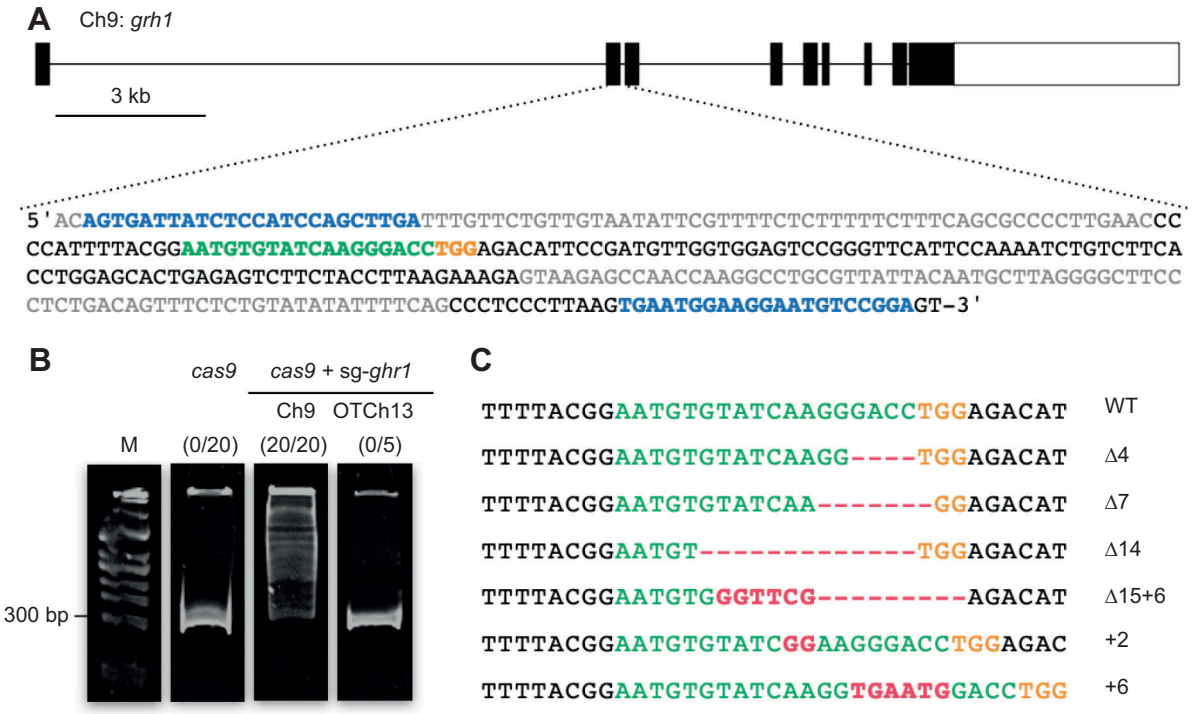

Fig. 4. Biallelic mutations of *ghr1* in *O. latipes* using CRISPR/Cas9. (A) Schematic representation of the genomic structure of *grh1* (ENSORLG00000004053). Coding exon regions are shown as solid boxes. The target sequence of sgRNA for *ghr1* is indicated by green letters, next to the NGG protospacer adjacent motif (PAM) sequence in orange letters. (B) Images from heteroduplex mobility assay (HMA) analysis of the efficiency of the CRISPR/Cas9 system and detection of off-target alterations. Representative gels from the HMA analysis are shown for embryos microinjected with only *cas9* and embryos microinjected with *cas9*+sg-*grh1* in amplifications to target the *ghr1* gene on chromosome 9 (Ch9) and potential off-target loci in chromosome 13 (OTCh13) (full-length gels are presented in Fig. S1). The number of embryos with biallelic mutations/total number of eggs injected is shown in parentheses. M, marker. (C) Subcloned sequences from the *cas9*-injected (WT) and *cas9*+sg-*ghr1*-injected embryos at F1. Red dashes and letters indicate the identified mutations. The size of indels is shown to the right of each mutated sequence.

After microinjection, eggs were assigned randomly to black or white backgrounds and sampled at 12 and 16 dph for each treatment. Firstly, for all individuals of each sampling time and treatment, the caudal fin was taken for genomic DNA (gDNA) extraction using conventional saline buffer extraction (Aljanabi and Martinez, 1997) to corroborate the biallelic mutations generate by the CRISPR/Cas9 system using HMA analysis. Conventional PCR analysis was performed with genomic DNA using primers: F 5′AGTGATTAT-CTCCATCCAGCTTGA3′ and R 5′TGAATGGAAGGAATGTC-CGGA3′ (Fig. 4A). The embryos that showed formation of heteroduplexes were considered to have biallelic mutations and were taken for analysis.

Screening for indels was performed in F1 fish. Biallelic mutant adult (F0) *O. latipes* were mated with wild-type medaka of the hi-medaka strain (WT). Genomic DNA was extracted from each F1 embryo for analysis of mutations by HMA, as described above. Mutant alleles in each embryo were determined by direct sequencing of the *ghr1* gene region.

Analysis of biallelic mutation phenotype in background adaptation

Oryzias latipes were sampled for chromatophore counting and standard body length measurements as described above. Melanophores and xanthophores were visualized on light magnifier while leucophores were detected by fluorescent light excitement (Kimura et al., 2014; Wada et al., 1998). Total chromatophore number was quantified from the dorsal region of the head.

RNA extraction and quantification

Total RNA was extracted from heads of individual embryos at 16 dph using 350 µl of TRIzol Reagent (Life Technologies), following the manufacturer's instructions. RNA quantification and purity were determined with a NanoDrop 2000 UV-vis spectrophotometer (Thermo Fisher Scientific). Samples were treated with DNase I (Sigma-Aldrich) to avoid genomic DNA contamination, using 1 µg of total RNA according to the manufacturer's instructions. cDNA synthesis was carried out with M-MLV enzyme (Promega, Madison, WI, USA) for 50 min at 37°C followed by 10 min at 70°C using random oligomers (hexamers) as reaction primers in a 10 µl final volume. Quantitative PCR (qPCR) reactions were conducted in a 10 µl final volume with 5 µl of 2× FastStart Universal SyBR Green Master mix (Roche, Basel, Switzerland), 1.5 µl of forward/reverse primer mix (Table S1; *ghr1*: 250 nmol l^{-1}; *ghr2*: 250 nmol l^{-1}; *rpl7*: 100 nmol l^{-1}), 2.5 µl of cDNA template and 1 µl of water. The amplification protocol consisted of an initial denaturation cycle at 95°C for 10 min, then 40 cycles of denaturation at 95°C for 30 s and annealing/elongation at 60°C for 30 s, followed by a melting curve from 65 to 95°C to detect possible non-specific PCR products. All primers were designed to give an amplicon size between 100 and 130 base pairs. Samples were run in duplicate and no-template controls were performed in every run for each primer pair. Raw fluorescence data from qPCR were exported from the Step One Plus Real-Time PCR System (Applied Biosystems, Waltham, MA, USA) to LinRegPCR (Amsterdam, The Netherlands) software and analysed to obtain the cycle threshold (CT) and PCR efficiency (Ramakers et al., 2003; Ruijter et al., 2009). PCR efficiencies for

all primer pairs were 90%. The subsequent quantification method was performed by using an efficiency-corrected method for relative expression (Pfaffl, 2001), normalizing against the *rpl7* gene (Zhang and Hu, 2006).

Statistical analysis

For morphological adaptation experiments in *C. dimerus*, both melanophore number and standard body length were analysed by repeated-measures (RM) ANOVA, while the number of ir-Sl cells, and ir-Sl cell and nuclear area were analysed by two-tailed Student's *t*-tests. *Post hoc* multiple comparisons by Holm–Šidák test were conducted after RM ANOVA. Melanophore number and standard length in wild-type *O. latipes* for the morphological adaptation experiment were analysed by two-way ANOVA followed by a Tukey's test for *post hoc* multiple comparison. Melanophore, leucophore and xanthophore number in morphological background adaption experiments on *ghr1*-mutated *O. latipes* were analysed separately for the 16 and 21 dph time points. At each time point, a nested ANOVA design was applied considering strain (*ghr1* mutated/*cas9* control), background (black/white) and their interaction as fixed factors, while experiment replication (two replications) was taken as a random factor nested in strain. A Tukey's *post hoc* test was applied whenever the interaction effect was statistically significant. ir-Sl cell number was analysed as explained above for *C. dimerus*. Correlation analysis between chromatophores and standard length was conducted by Pearson's test. Standard length comparison between *ghr1*-mutated and *cas9*/control *O. latipes* was conducted by a two-way ANOVA considering strain and background as factors. Fold-change and statistical analysis of qPCR were performed using FgStatistics interface (http://sites.google.com/site/fgStatistics/), based on the Relative Expression Software Tool (REST) (Pfaffl, 2001). All *P*-values were corrected for multiple comparisons in order to avoid family-wise error rate increments. Data are presented as means±s.e.m. For parametric tests, data were checked for homoscedasticity and normality assumptions.

RESULTS

Cichlasoma dimerus

Background colour effect on melanophore number

First, we examined the onset of background colour adaptation during development as the moment when the fish is first able to sense and respond to different backgrounds. Thus, we started the background colour adaptation experiment immediately after egg fertilization. From 15 dph, the number of melanophores was greater in larvae raised in black than in white tanks (white 185±11 versus black 248±23; P=0.032) and this difference was increased at 21 dph (white 188±11 versus black 264±21; P=0.014) and 30 dph (white 209±8 versus black 327±27; P<0.001; Fig. 1B–D). No differences were observed at 10 dph (white: 192±11 versus black: 216±16; P>0.05; Fig. 1D). Additionally, standard length was not different between treatments at any time (P>0.05; Fig. 1E).

Background colour effect on ir-Sl cells

As background colour adaptation was present from 15 dph, we asked whether these changes in melanophore number in larvae adapted to white and black backgrounds could be related to changes in the pituitary Sl cells. The immunohistochemistry assays revealed a higher number of ir-Sl cells in black-adapted larvae at 30 dph (Fig. 2A–C; P=0.009). Both cell area and nuclear area of ir-Sl cells were larger in larvae from black backgrounds (P=0.015 and P=0.004, respectively; Fig. 2A,B,D,E).

Oryzias latipes

Background colour effect on chromatophore number

To test whether Ghr1, the putative Sl receptor, is involved in colour background adaptation, we used *O. latipes*. Thus, we first had to evaluate whether *O. latipes*, like *C. dimerus*, is able to adapt to white and black backgrounds from early stages of development (Fig. 3A). *Oryzias latipes* larvae raised in black tanks presented a higher number of melanophores than those raised in white tanks at 12 dph (white 46±3 versus black 63±4; P=0.016) and 16 dph (white 38±4 versus black 96±12; P<0.001), while no differences were observed at 9 dph (Fig. 3B–D). Standard length was no different for fish in the two treatments (P>0.05; Fig. 3E).

Background colour effect on chromatophore number in *ghr1* biallelic mutant larvae

Once we had verified the background colour adaptation in *O. latipes* larvae, our next step was to analyse the participation of *ghr1* in this process by generating biallelic mutations of this gene (Fig. 4). We obtained F0 individuals with biallelic mutations on *ghr1* (also known as crispants) with a 100% efficiency of injected eggs as determined by HMA (Fig. 4B). We confirmed the presence of indels on exon 2 of *ghr1* (Fig. 4A) by the presence of multiple bands of heteroduplex (Fig. 4B), and later confirmed this by sequencing (Fig. 4C). Additionally, no indels on potential off-target sites were observed, as can be seen by the presence of a single band in the HMA assay (Fig. 4B).

As *ghr1* is a paralogue of *ghr2*, which has been demonstrated to participate in somatic growth, we analysed firstly the standard length of biallelic *ghr1* mutant larvae raised in white and black backgrounds (Fig. 5A). We observed that biallelic *ghr1* mutants showed a decrease in somatic growth compared with wild-type larvae, independently of the background colour (Fig. 5B). Additionally, we observed no differences in chromatophore colour between treatments and strains. Visualization with incident light showed black melanophores, orange–cream leucophores and orange xanthophores, while observation with transmitted light showed same appearance for melanophores and xanthophores but a different colour (brownish) for leucophores (Fig. 5C–F).

Then, we subjected biallelic *ghr1*-mutated *O. latipes* larvae to background colour adaptation experiments to evaluate the involvement of *ghr1* in this process (Fig. 5A). No differences in number of each chromatophore type were found between mutant and wild-type *O. latipes* at 9 dph in response to black and white backgrounds (Fig. 6A–C; $P_{strain\times background}$>0.05). However, differences were observed at 16 dph, where the interaction effect between strain and background was significant for all chromatophores ($P_{strain\times background}$<0.001; Fig. 6A–C). Specifically, colour background adaptation was observed in control *cas9 O. latipes* (strain injected only with *cas9*), in which black-adapted embryos presented more melanophores and leucophores than white-adapted ones (P<0.001; Fig. 6A,B). In contrast, *ghr1* biallelic mutants failed to adapt to the background as melanophore and leucophore numbers between black and white treatments were not different (P>0.05; Fig. 6A,B).

However, the number of xanthophores was not different between black- and white-adapted fish at 9 dph (Fig. 6C; background effect: P>0.05) for both *ghr1* biallelic mutants and *cas9*-injected strains ($P_{strain\times background}$>0.05), although *ghr1*-mutated *O. latipes* presented a lower quantity of xanthophores (strain effect: P<0.001). At 16 dph, there was a background×line interaction effect ($P_{strain\times background}$< 0.009) where black-adapted biallelic *ghr1*-mutated *O. latipes* individuals presented a lower number of xanthophores than white-adapted ones (P=0.034).

Journal of Experimental Biology (2020) 223, jeb230375. doi:10.1242/jeb.230375

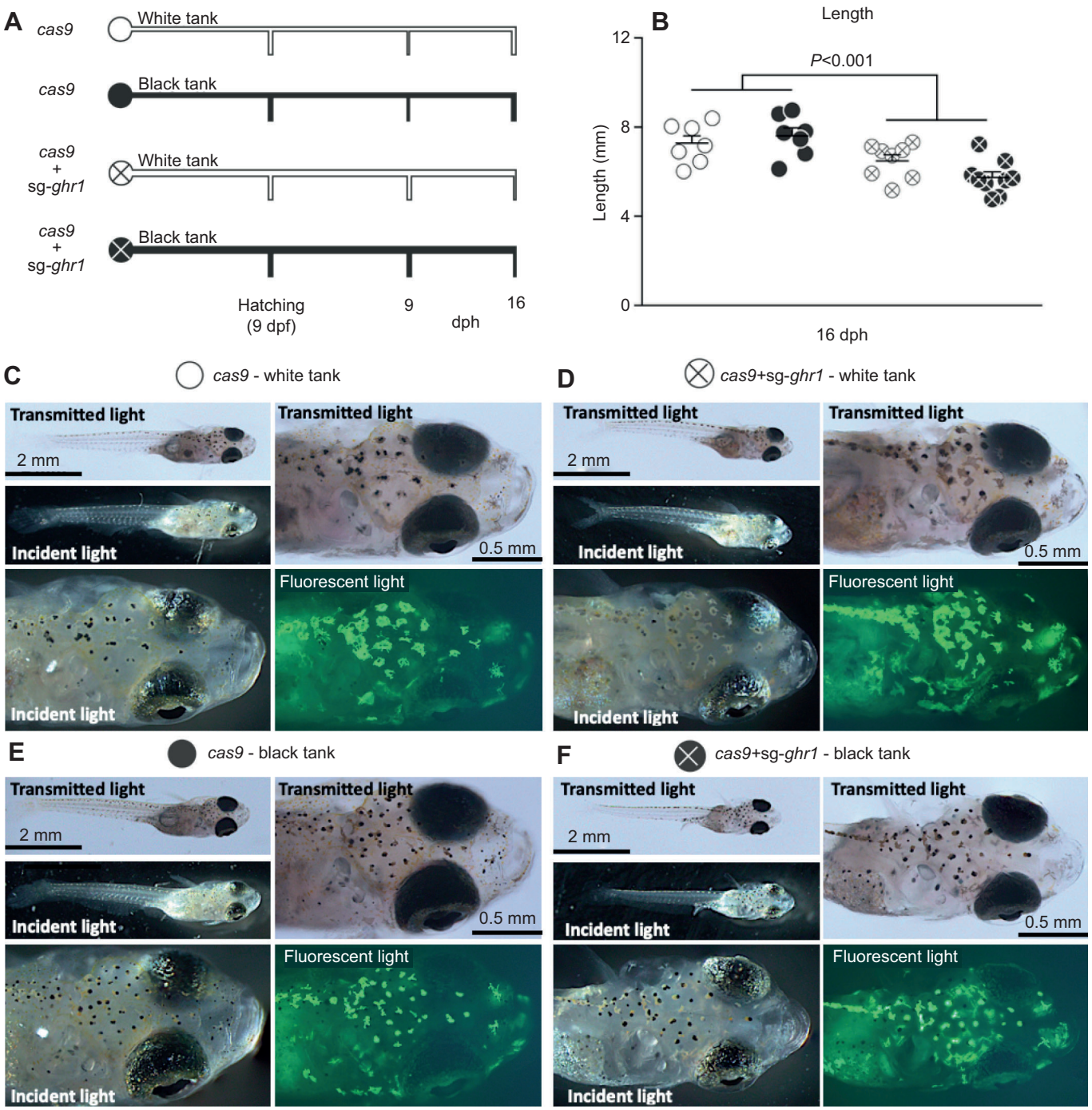

Fig. 5. Background adaptation of individuals with biallelic mutations of *grh1*. (A) Schematic representation of the experimental design; embryos microinjected with *cas9* or *cas9*+sg-*grh1* were exposed from fertilization until 16 dph to white or black tank environments. Hatching occurred at 9 dpf. Samples were collected at 9, 12 and 16 dph. (B) Standard length of individuals from the white tank (*cas9*, white circles, *n*=7; *cas9*+sg-*grh1*, crossed-out white circles, *n*=8) and black tank (*cas9*, black circles, *n*=7; *cas9*+sg-*grh1*, crossed-out black circles, *n*=8) at 16 dph. (C–F) Photomicrographs with different light point exposure and wavelength to observe the types of chromatophores in individuals exposed to a white tank (*cas9*, white circles, C; *cas9*+sg-*grh1*, crossed-out white circles, D) or a black tank (*cas9*, black circles, E; *cas9*+sg-*grh1*, crossed-out black circles, F) at 16 dph.

Additionally, we detected a strong positive correlation between melanophore and leucophore number (r=0.842, P<0.0001; Fig. 6D). No association between xanthophores and melanophores or leucophores was found (r=0.16, P=0.4 and r=0.25, P=0.22, respectively). It is worth mentioning that 9 dph *O. latipes* larvae reared in black backgrounds, unlike those from the experiment shown in Fig. 3, presented more melanophores and leucophores than white-adapted fish (main effect P<0.001; Fig. 6A,B) both in biallelic *ghr1*-mutated and *cas9*-injected *O. latipes* (interaction effect P>0.05).

Lastly, we analysed the correlation between total length and the number of different chromatophores. Weak correlations of length with melanophores and leucophores but not with xanthophores was observed (Fig. S2).

Journal of Experimental Biology (2020) 223, jeb230375. doi:10.1242/jeb.230375

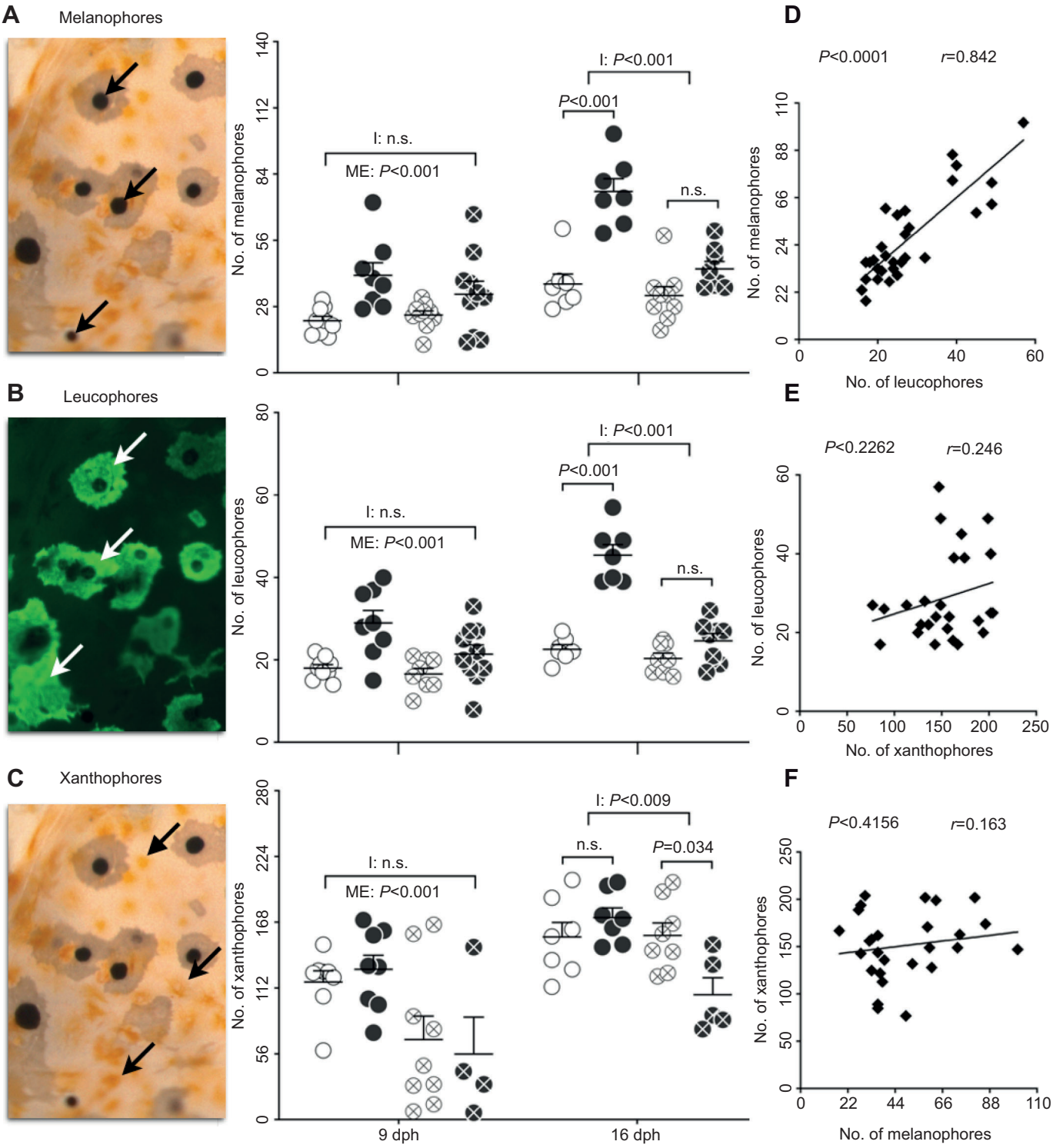

Fig. 6. Number of chromatophores in individuals with biallelic mutations under background adaptation. (A–C) Photomicrographs (left) of melanophores (A), leucophores (B) and xanthophores (C) (arrows) and the number of each chromatophore (right) in the head of individuals reared in a white tank (*cas9*, white circles; *cas9*+sg-*grh1*, crossed-out white circles) or black tank (*cas9*, black circles; *cas9*+sg-*grh1*, crossed-out black circles) at 9 and 16 dph. Sample size from left to right: melanophores n=9, 9, 9, 10, 7, 7, 9, 8; leucophores n=9, 8, 7, 10, 7, 7, 8, 8; and xanthophores n=8, 8, 8, 4, 7, 7, 8, 5. (D–F) Pearson's correlation coefficients between melanophores and leucophores (D), leucophores and xanthophores (E), and xanthophores and melanophores (F).

It is worth noting that the lack of background adaptation in *ghr1*-mutated *O. latipes* can arguably be nothing but a side effect of its reduced somatic growth (Fig. 5B). To evaluate this hypothesis, we inspected in detail data on growth and melanophore number from wild-type *O. latipes* (Fig. 3) and compared it with data for *ghr1*-mutated *O. latipes* (Fig. 6). As before, lack of background adaptation was observed at 16 dph in mutated *ghr1 O. latipes*. At this time, the fish were 6 mm long and showed no statistical

Journal of Experimental Biology (2020) 223, jeb230375. doi:10.1242/jeb.230375

differences in the number of leucophores and melanophores. In contrast, wild-type *O. latipes* of equivalent size (5.5 mm long) were observed at 12 dph, where black-adapted fish presented more melanophores than white-adapted fish (Fig. 3). These data show that, once the size effect on melanophore number is discarded, only *ghr1*-mutated *O. latipes* is unable to adapt to black backgrounds.

Background colour effect on ir-Sl cells in *ghr1* biallelic mutant larvae

Finally, we asked whether the lack of background colour adaptation seen at 16 dph in *ghr1* biallelic mutant *O. latipes* was related to Sl production. Thus, we carried out immunohistochemistry assays on 16 dph larvae (Fig. 7A–D). We found no difference between *ghr1* mutants and *cas9*-injected *O. latipes* in the number of ir-Sl cells, or their cell or nuclear size ($P_{strain\times background}$>0.05; Fig. 7E–G). However, as previously observed in *C. dimerus*, black-adapted *O. latipes* from both lines presented more ir-Sl cells (P=0.008) with a larger cell and nuclear size (P<0.001) than white-adapted ones (Fig. 7E–G).

Background colour effect on ir-Gh cells and Gh receptors in *ghr1* biallelic mutant larvae

Given the high structural similarity and phylogenetic relationship between Sl and Gh, we next evaluated the number of ir-Gh cells in the pituitary gland of 16 dph *O. latipes* (Fig. 8C–F). No differences were observed between the number of ir-Gh cells (Fig. 8G), ir-Gh cell area (Fig. 8H) and ir-Gh nuclear area (Fig. 8I) in fish reared with black and white backgrounds and between fish strains.

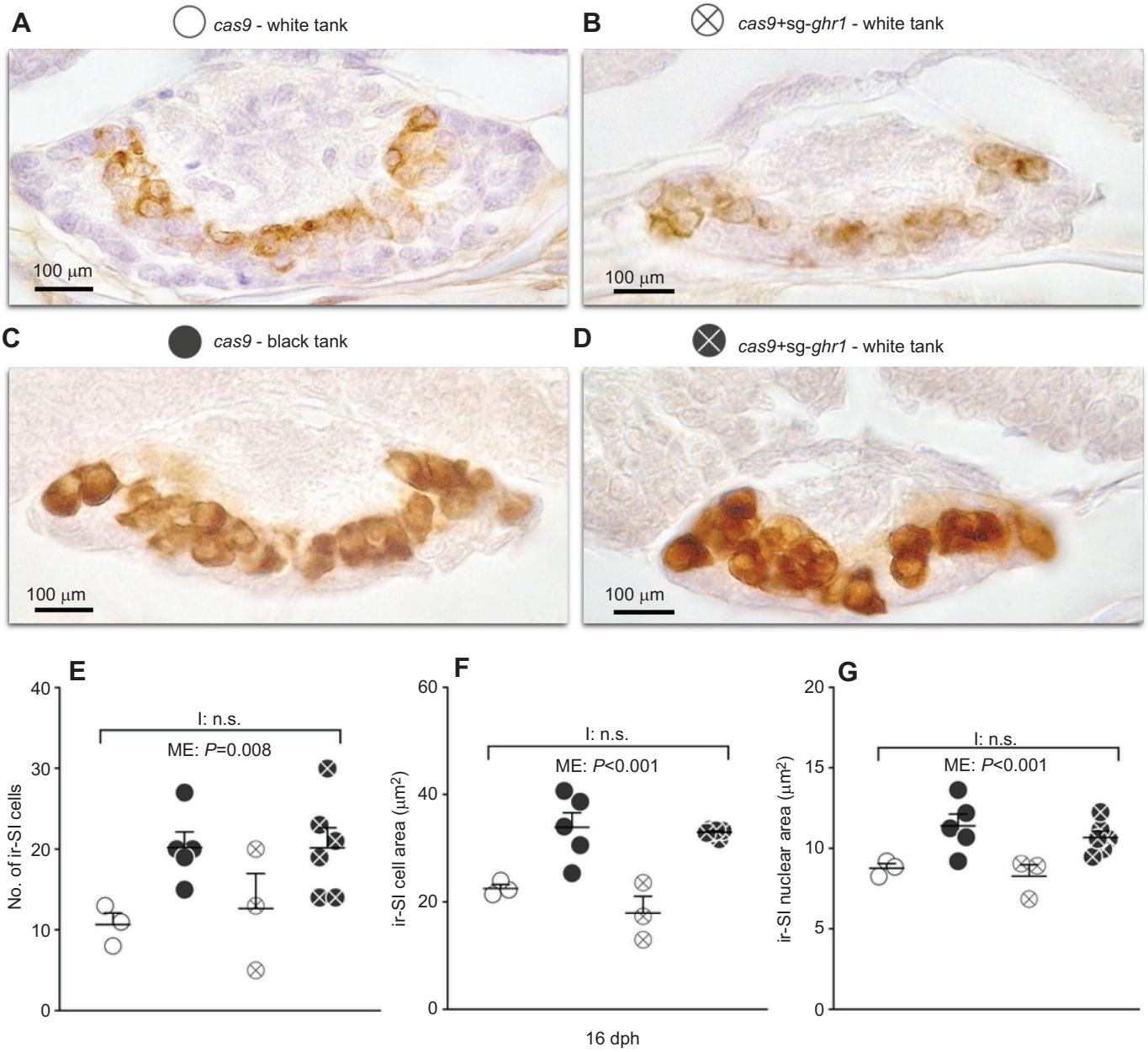

Fig. 7. Sl response to background adaptation of individuals with biallelic mutations of *grh1*. Transverse sections of the pituitary gland with ir-Sl cells of individuals exposed to a white tank (*cas9*, white circles, *n*=3, A; *cas9*+sg-*grh1*, crossed-out white circles, *n*=5, B) or a black tank (*cas9*, black circles, *n*=3, C; *cas9*+sg-*grh1*, crossed-out black circles, *n*=6, D) at 16 dph. (E–G) Number of ir-Sl cells (E), ir-Sl cell area (F) and ir-Sl nuclear area (G) of individuals from each treatment at 16 dph.

Journal of Experimental Biology (2020) 223, jeb230375. doi:10.1242/jeb.230375

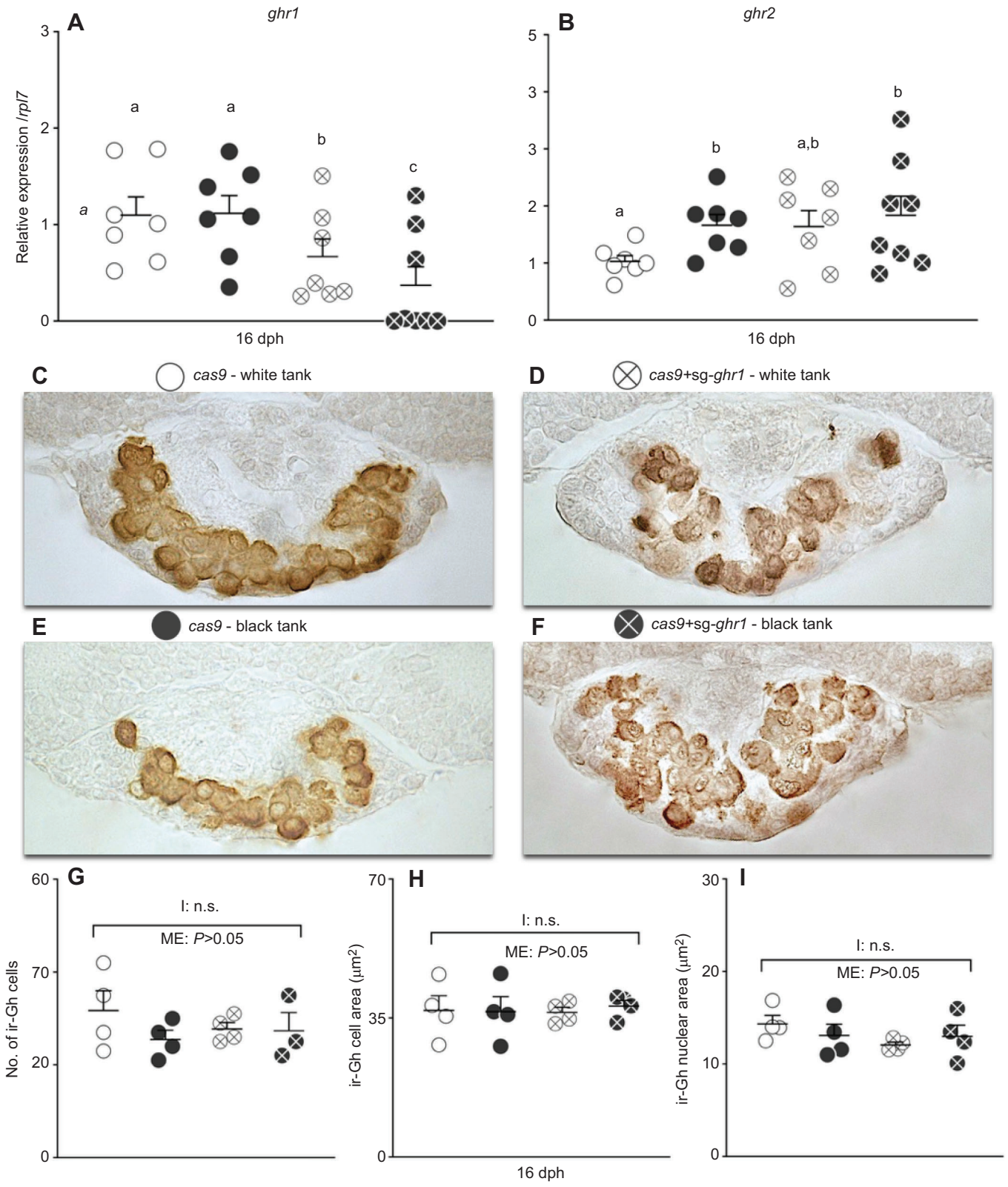

Fig. 8. Relative expression of growth hormone receptors and growth hormone response to background adaptation of individuals with biallelic mutations on *grh1*. Transcript abundance profiles of *ghr1* (A) and *ghr2* (B) from individuals reared in a white tank (cas9, white circles, *n*=7; cas9+sg-grh1, crossed-out white circles, *n*=7) or a black tank (cas9, black circles, *n*=7; cas9+sg-grh1, crossed-out black circles, *n*=8) at 16 dph. Gene expression levels are expressed relative to the white tank *cas9* (white circles) group and normalized to *rpl7*. Different letters indicate statistically significant differences between treatments. (C–E) Transverse sections of the pituitary gland with ir-growth hormone (Gh) cells from individuals exposed to a white tank (*cas9*, white circles, *n*=4, C; *cas9*+sg-*grh1*, crossed-out white circles, *n*=4, D) or a black tank (*cas9*, black circles, *n*=4, E; *cas9*+sg-*grh1*, crossed-out black circles, *n*=3, F) at 16 dph. (G–I) Number of ir-Gh cells (G), ir-Gh cell area (H) and ir-Gh nuclear area (I) in individuals from each treatment at 16 dph.

Journal of Experimental Biology (2020) 223, jeb230375. doi:10.1242/jeb.230375

Additionally, *ghr1* mRNA levels were lower in *ghr1* mutant *O. latipes* (P=0.003), with no differences between individuals from black and white treatments in *cas9* strain (Fig. 8A). In contrast, *ghr2* mRNA expression was higher in black-adapted fish of the *cas9* strain (P=0.005), while this difference was not detected in *ghr2*-mutated fish (P=0.326; Fig. 8B).

DISCUSSION

Background adaptation has been widely studied in fish as well as in many other vertebrate species (Aspengren et al., 2008; Leclercq et al., 2010; Sköld et al., 2016; Sugimoto, 2002). Nevertheless, most studies were focused on physiological other than morphological changes; that is to say, changes that affect pigment aggregation or dispersion that occurs over short periods of time but not variation in the number of chromatophores on the skin, a process that involves both cell differentiation and proliferation and is referred to as morphological adaptation (Sugimoto et al., 2000; Sugimoto, 2002). Although several endocrine and nervous system mechanisms have been proposed to regulate morphological adaptation in adult fish, including a central role of Sl (Fukamachi et al., 2004), the onset of such a process during development remained unexplored until now. Here, we present clear evidence on the occurrence of morphological background adaptation at early developmental stages in two fish species concomitant with variation in Sl. Moreover, as far as we know, this is the first work that analyses the mutation of *ghr1*, a putative Sl receptor, demonstrating that morphological background adaptation in the first stages of development is dependent upon this Gh receptor.

We first aimed to determine when fish are able to adapt to the background. Results from *C. dimerus* indicate that the mechanisms by which adaptation takes place must be present early in larvae stages. By 15 dph, the hypothalamic neuropeptide melanin-concentrating hormone (Mch), the *pars* intermedia pituitary hormones melanocyte-stimulating hormone (Msh) and Sl are already being expressed in *C. dimerus* (Pandolfi et al., 2001, 2003) – hormones that have been demonstrated to regulate both morphological and physiological changes in adult fish (Cánepa et al., 2006, 2012; Sköld et al., 2016; Sugimoto, 2002; Zhu and Thomas, 1997). This co-occurrence in time between background adaptation and the presence of these hormones shows that skin pigmentation-regulating mechanisms are active from an early stage of development. A previous study carried out in rainbow trout showed that physiological background adaptation is present at early stages in ontogeny and that it is dependent upon sympathetic innervations, but not on Mch or Msh, both factors being present before adaptation took place (Suzuki et al., 1997). This conclusion was based on the fact that physiological background adaptation occurred at 10 dph, but neither Mch nor Msh expression was altered by a black or white background until 28 dph. Unfortunately, the authors did not analyse whether morphological background adaptation occurred after 28 dph. Although we did not evaluate Mch and Msh in this work, we detected an increment in Sl-producing cells along with a larger nuclear and cell size in individuals reared in black compared with white backgrounds. Even though we were not able to measure Sl levels in plasma, these facts are indicative of an increment of Sl in the organism. Moreover, the number of Gh-producing cells, as well as ir-Gh cell and nuclear area were not affected by background or *O. latipes* strain, which suggest that Gh, unlike Sl, is not involved in morphological background adaptation. Together, the increment in melanophores at 15 dph in black-adapted fish agrees with the hypothesis that Sl is involved in background colour adaptation, as in adult *C. dimerus* (Cánepa et al., 2006, 2012).

The function of *ghr1* is not completely understood in fish. As stated above, it was first described as a Sl receptor in salmonids, but later *in vitro* studies in other fish species demonstrated that Ghr1 responds to Gh, but not to Sl (Chen et al., 2011). These contradictory results can be attributable to species-specific differences due to divergence and subfunctionalization. Thus, we hypothesized that if Ghr1 is a Sl receptor, as proposed for salmonids (Fukada et al., 2005), medaka and other fish species (Cánepa et al., 2012; Fukamachi et al., 2005; Fukamachi and Meyer, 2007), and considering that *ci* medaka, which lacks a functional α-Sl, presents alterations in chromatophore proliferation and morphogenesis, a *ghr1* mutation in fish should result in altered background adaptation and/or chromatophore production. Therefore, we generated CRISPR/Cas9 mutants for *ghr1* in *O. latipes*, as this technique is not available in *C. dimerus*. Our results showed that wild-type *O. latipes* is able to adapt to black backgrounds at 16 dph, which indicates that the processes that allow for background adaptation are present before 16 dph and after 9 dph. Interestingly, morphological adaptation to a black background is severely diminished for melanophores and completely abolished for leucophores in *ghr1*-deficient *O. latipes* when compared with control/*cas9* ones at 16 dph. Thus, the lack of morphological adaptation in *ghr1*-deficient *O. latipes* is in agreement with the hypothesis that Ghr1 is the Sl receptor. This fact does not exclude the possibility that *ghr2*, the *ghr1* paralogue, can mediate other biological functions of Sl. Indeed, we did not observe an effect of *ghr1* mutations on Sl-producing cells, which may suggest that Sl is binding to other receptors as well or the absence of a negative feedback loop to this endocrine pathway. In relation to that, we observed that *ghr2* but not *ghr1* is upregulated in black-adapted *O. latipes* for the control cas9 strain, but it disappears in *ghr1* biallelic mutants. Nevertheless, the lack of effect of background on *ghr1* expression in *cas9 O. latipes* larvae may be due to technical issues, as in this work we started from RNA extracted from whole head, whereas those studies in which *ghr1* was upregulated were conducted in isolated scales from adults (Cánepa et al., 2012). Interestingly, *ghr1* mRNA expression decreased in *ghr1* mutant *O. latipes*.

To our knowledge, this is the first study to report the functional role of *ghr1* in background adaptation. However, the role of Sl in body pigmentation has been studied in *ci* medaka, a mutant strain which lacks a functional Sl. These *ci* medaka showed phenotypic alterations related to proliferation and differentiation of chromatophores (Fukamachi et al., 2004); in particular, they present a grey body colour caused by an increase in the number and size of white leucophores and a decrease in the number of orange xanthophores, with no differences in melanophore number. If Ghr1 was the Sl receptor, we would expect that the *ci* medaka and *ghr1* mutant *O. latipes* phenotypes to be similar. In fact, this was the case except for leucophores. Our results show that *ghr1* mutant *O. latipes* contain fewer xanthophores than control individuals, no variation in melanophores and, unlike *ci* medaka, no variation in leucophore number. Interestingly, the colour of leucophores in *ghr1* mutants is orange-cream, as in control individuals, while in *ci* medaka, they are white. If Ghr1 was the Sl receptor, a possible explanation for this discrepancy could be the methodology of mutant strain generation. The genetic background of the *ci* medaka line may be very different from that of the strain used in these studies, where the *ghr1* mutant *O. latipes* was designed specifically.

However, as Ghr1 is a Gh receptor paralogue, it is expected that this receptor maintains functions related to Gh function such as growth. Indeed, we showed that somatic growth is reduced in *ghr1* mutated *O. latipes*. This result along with the lack of morphological background adaptation in this *ghr1 O. latipes* strain is in agreement

with studies carried out in *ci* medaka that overexpress Gh ectopically (Komine et al., 2016). This *ci* medaka showed a larger body size, as expected from overexpressing Gh, and surprisingly a higher number of melanophores in the skin than control fish (Komine et al., 2016), although to a lesser extent than in *ci* medaka that overexpress Sl ectopically (Fukamachi et al., 2009). Taken together, these facts may suggest crosstalk between Gh and Sl with Ghr1, although an interaction hormone–receptor assay is needed to test this hypothesis. In this sense, a study carried out in zebrafish has demonstrated an interaction between Gh and Ghr1 when evaluated by reporter gene assays but a lack of Sl–Ghr1 interaction (Chen et al., 2011). In contrast, binding assays in salmonids have shown a high-affinity interaction between Sl and Ghr1 (Fukada et al., 2005), which suggests that the Sl–Ghr1 interaction may be species specific.

Finally, it should be mentioned that although Ghr1 regulates morphological background adaptation, it does not affect normal melanophore and leucophore production, as larvae present a normal colour appearance with no evident difference in the amount of these chromatophores between *ghr1*-mutated and *cas9 O. latipes*. Thus, how is it possible that Ghr1 is able to regulate morphological adaptation without affecting the production of chormatophores? A potential explanation is that Ghr1 is involved in chromatophore survival. A number of studies on mammalian models have demonstrated survival and protective effects of Gh in immune cells through Ghr (Jeay et al., 2002), and as Ghr1 is a Gh receptor paralogue, this function may remain for Ghr1. As stated before, the number of chromatophores in the skin is a result of production by proliferation/differentiation and elimination by apoptosis (Sugimoto et al., 2000; Sugimoto, 2002). In this context, high levels of Sl induced by long-term adaptation to black backgrounds would activate Ghr1 and stimulate chromatophore survival, but when Ghr1 is mutated, this protective effect would be lost and as a consequence the number of chromatophores would not increase: all newly produced chromatophores would eventually be eliminated by apoptosis. Our results show that black-adapted fish present more Sl-producing cells with a larger cell and nuclear size, which indirectly suggests higher levels of Sl, and gives support to the survival hypothesis. However, a better method of Sl quantification should be used to this purpose. Further experiments should be developed to test this hypothesis.

Both *ghr1*-mutated *O. latipes* and *ci* medaka lack of morphological adaptation for leucophores (Fukamachi et al., 2004). In this species, it was reported that adaptation to white backgrounds results in a higher number of leucophores in the trunk of the body (Sugimoto et al., 2000), but in *ci* medaka, this increment does not take place (Fukamachi et al., 2004). In our experiments, the number of leucophores increased in wild-type black-adapted *O. latipes*, but this increment was not observed in *ghr1*-mutated *O. latipes*. Besides the opposite response of leucophores to background adaptation, it is important to note that both *ci* medaka and *ghr1*-mutated *O. latipes* showed no morphological background adaptation, which suggests that both Sl and Ghr1 play a role in leucophore number regulation in long-term background adaptation. The opposite response in the number of leucophores in wild-type fish to long-term background adaptation could be explained by the region in which they were quantified. In the experiments carried out by Sugimoto et al. (2000) in *ci* medaka, leucophores were measured in the trunk of adult fish, while the results presented in this work were quantified as the total amount of chromatophores at larvae stages on the dorsal side of the head. Additionally, head melanophores and leucophores appeared to be very close in space. In this sense, we observed a strong positive correlation in the number of head melanophores and leucophores. This feature along with a similar response to long-term background adaptation suggests a common regulatory mechanism dependent upon *ghr1* for melanophores and leucophores. Interestingly, recent research performed on zebrafish has demonstrated the existence of transdifferentiation from xanthophores and melanophores to a leucophore-like chromatophores named xantholeucophores and melanoleuchophores, respectively (Lewis et al., 2019). They postulated that xantholeucophores are similar to medaka leucophores both structurally and physiologically as they respond to light exposure by aggregating the pigment-containing vesicles. However, melanoleucophores contain structurally different pigment-containing organelles and behave similar to melanophores in response to light exposure by dispersing the pigment (Lewis et al., 2019). Considering our results where melanophores and leucophores respond similarly to long-term background adaptation, this raises the question whether there is any possibility of transdifferentiation between melanophores and leucophores in medaka as well. However, it should be noted that the location of those leucophore-like cells from zebrafish is restricted to the border of the anal and caudal fins of adult fish, while medaka leucophores are present all around the body. More importantly, leucophores analysed in this work are located in the dorsal region of the head, where it is known that during development melanophores and leucophores are highly associated (Lynn Lamoreux et al., 2005). In this sense, more research is needed to unravel this possibility and to determine whether xantholeucophores and melanoleucopores present morphological background adaptation.

The early onset of background adaptation is clear in both *C. dimerus* and *O. latipes*, as determined by the higher number of melanophores in black-adapted fish. However, the medaka strain in which the experiments were conducted was hi-medaka, a strain known to have a variable amount of amelanic melanophores but normal leucophores and xanthophores. This fact may obscure data interpretation derived from melanophores. For this reason, the involvement of *ghr1* in morphological background adaptation is mainly supported by the lack of leucophore background adaptation in *ghr1*-mutated medaka. Nevertheless, the number of melanophores was mirrored by the behaviour of leucophore numbers with a high statistical correlation, which in turn, despite the possible presence of amelanic melanophores, validates the involvement of *ghr1* in melanophore background adaptation.

In summary, in this work we present clear evidence of the role of *ghr1* in the regulation of morphological colour background adaptation early during development.

Acknowledgements
We are especially grateful to Dr Shoji Fukamachi, who not only inspired our study through his work but also contributed feedback on this manuscript. We thank NBRP Medaka (https://shigen.nig.ac.jp/medaka/) for providing the hi-medaka (strain ID: MT835).

Competing interests
The authors declare no competing or financial interests.

Author contributions
Conceptualization: T.H.D., J.I.F., P.G.V.; Methodology: T.H.D., D.C.C.-C., J.I.F.; Formal analysis: T.H.D.; Investigation: T.H.D., D.C.C.-C., C.S., A.B.; Resources: J.I.F., P.G.V.; Writing - original draft: T.H.D., P.G.V.; Writing - review & editing: T.H.D., J.I.F., P.G.V.; Visualization: T.H.D., D.C.C.-C.; Supervision: P.G.V., J.I.F.; Project administration: P.G.V.; Funding acquisition: J.I.F., P.G.V.

Funding
This study was supported by the Universidad de Buenos Aires (grant 20020160100110BA to P.G.V.), Consejo Nacional de Investigaciones Científicas y Técnicas (CONICET; PIP 2014–2016: 11220130100501CO to P.G.V.) and Agencia Nacional de Promoción Científica y Tecnológica (grant 2501/15 to J.I.F.). T.H.D. and D.C.C.-C. were supported by a PhD scholarship from the Consejo Nacional de Investigaciones Científicas y Técnicas (CONICET). J.I.F. and P.G.V. are members of the Scientific and Technological Researcher Career (CIC) at CONICET.

Supplementary information

Supplementary information available online at
https://jeb.biologists.org/lookup/doi/10.1242/jeb.230375.supplemental

References

Aljanabi, S. M. and Martinez, I. (1997). Universal and rapid salt-extraction of high quality genomic DNA for PCR-based techniques. *Nucleic. Acids. Res.* **25**, 4692-4693. doi:10.1093/nar/25.22.4692

Ansai, S. and Kinoshita, M. (2014). Targeted mutagenesis using CRISPR/Cas system in medaka. *Biol. Open.* **3**, 362-371. doi:10.1242/bio.20148177

Aspengren, S., Hedberg, D., Sköld, H. N. and Wallin, M. (2008). New insights into melanosome transport in vertebrate pigment cells. *Int. Rev. Cell. Mol. Bio.* **272**, 245-302. doi:10.1016/S1937-6448(08)01606-7

Astola, A., Pendón, C., Ortíz, M. and Valdivia, M. M. (1996). Cloning and expression of somatolactin, a pituitary hormone related to growth hormone and prolactin from gilthead seabream, *Sparus aurata*. *Gen. Comp. Endocr.* **104**, 330-336. doi:10.1006/gcen.1996.0178

Benedet, S., Björnsson, B. T., Taranger, G. L. and Andersson, E. (2008). Cloning of somatolactin alpha, beta forms and the somatolactin receptor in Atlantic salmon: seasonal expression profile in pituitary and ovary of maturing female broodstock. *Reprod. Biol. Endocrin.* **6**, 42. doi:10.1186/1477-7827-6-42

Cánepa, M. M., Pandolfi, M., Maggese, M. C. and Vissio, P. G. (2006). Involvement of somatolactin in background adaptation of the cichlid fish *Cichlasoma dimerus*. *J. Exp. Zool. Part. A* **305**, 410-419. doi:10.1002/jez.a.273

Cánepa, M. M., Zhu, Y., Fossati, M., Stiller, J. W. and Vissio, P. G. (2012). Cloning, phylogenetic analysis and expression of somatolactin and its receptor in *Cichlasoma dimerus*: Their role in long-term background color acclimation. *Gen. Comp. Endocr.* **176**, 52-61. doi:10.1016/j.ygcen.2011.12.023

Castañeda Cortés, D. C., Padilla, L. F. A., Langlois, V. S., Somoza, G. M. and Fernandino, J. I. (2019). The central nervous system acts as a transducer of stress-induced masculinization through corticotropin-releasing hormone B. *Development* **146**, dev172866. doi:10.1242/dev.172866

Chen, M., Huang, X., Yuen, D. S. H. and Cheng, C. H. K. (2011). A study on the functional interaction between the GH/PRL family of polypeptides with their receptors in zebrafish: evidence against GHR1 being the receptor for somatolactin. *Mol. Cell. Endocrinol.* **337**, 114-121. doi:10.1016/j.mce.2011.02.006

Fujii, R. (1993). Cytophysiology of fish chromatophores. In *International Review of Cytology* (ed. W. Kwang, M. F. Jeon and J. Jonathan), pp. 191-255. San Diego, USA: Academic Press.

Fukada, H., Ozaki, Y., Pierce, A. L., Adachi, S., Yamauchi, K., Hara, A., Swanson, P. and Dickhoff, W. W. (2004). Salmon growth hormone receptor: molecular cloning, ligand specificity, and response to fasting. *Gen. Comp. Endocr.* **139**, 61-71. doi:10.1016/j.ygcen.2004.07.001

Fukada, H., Ozaki, Y., Pierce, A. L., Adachi, S., Yamauchi, K., Hara, A., Swanson, P. and Dickhoff, W. W. (2005). Identification of the salmon somatolactin receptor, a new member of the cytokine receptor family. *Endocrinology.* **146**, 2354-2361. doi:10.1210/en.2004-1578

Fukamachi, S. and Meyer, A. (2007). Evolution of receptors for growth hormone and somatolactin in fish and land vertebrates: lessons from the lungfish and sturgeon orthologues. *J. Mol. Evo.* **65**, 359-372. doi:10.1007/s00239-007-9035-7

Fukamachi, S., Sugimoto, M., Mitani, H. and Shima, A. (2004). Somatolactin selectively regulates proliferation and morphogenesis of neural-crest derived pigment cells in medaka. *Proc. Natl. Acad. Sci. USA* **101**, 10661-10666. doi:10.1073/pnas.0401278101

Fukamachi, S., Yada, T. and Mitani, H. (2005). Medaka receptors for somatolactin and growth hormone: phylogenetic paradox among fish growth hormone receptors. *Genetics* **171**, 1875-1883. doi:10.1534/genetics.105.048819

Fukamachi, S., Yada, T., Meyer, A. and Kinoshita, M. (2009). Effects of constitutive expression of somatolactin alpha on skin pigmentation in medaka. *Gene* **442**, 81-87. doi:10.1016/j.gene.2009.04.010

Hwang, W. Y., Fu, Y., Reyon, D., Maeder, M. L., Kaini, P., Sander, J. D., Joung, J. K., Peterson, R. T. and Yeh, J.-R. J. (2013). Heritable and precise zebrafish genome editing using a CRISPR-Cas system. *PLoS ONE* **8**, e68708. doi:10.1371/journal.pone.0068708

Jeay, S., Sonenshein, G. E., Postel-Vinay, M.-C., Kelly, P. A. and Baixeras, E. (2002). Growth hormone can act as a cytokine controlling survival and proliferation of immune cells: new insights into signaling pathways. *Mol. Cell. Endocrinol.* **188**, 1-7. doi:10.1016/S0303-7207(02)00014-X

Johnson, L. L., Norberg, B., Willis, M. L., Zebroski, H. and Swanson, P. (1997). Isolation, characterization, and radioimmunoassay of Atlantic halibut somatolactin and plasma levels during stress and reproduction in flatfish. *Gen. Comp. Endocr.* **105**, 194-209. doi:10.1006/gcen.1996.6821

Kakisawa, S., Kaneko, T., Hasegawa, S. and Hirano, T. (1995). Effects of feeding, fasting, background adaptation, acute stress, and exhaustive exercise on the plasma somatolactin concentrations in rainbow trout. *Gen. Comp. Endocr.* **98**, 137-146. doi:10.1006/gcen.1995.1054

Kaneko, T. and Hirano, T. (1993). Role of prolactin and somatolactin in calcium regulation in fish. *J. Exp. Biol.* **184**, 31-45.

Kawauchi, H. and Sower, S. A. (2006). The dawn and evolution of hormones in the adenohypophysis. *Gen. Comp. Endocr.* **148**, 3-14. doi:10.1016/j.ygcen.2005.10.011

Kimura, T., Nagao, Y., Hashimoto, H., Yamamoto-Shiraishi, Y.I., Yamamoto, S., Yabe, T., Takada, S., Kinoshita, M., Kuroiwa, A. and Naruse, K. (2014). Leucophores are similar to xanthophores in their specification and differentiation processes in medaka. *Proc. Natl. Acad. Sci. USA* **111**, 7343-7348.

Kinoshita, M., Kani, S., Ozato, K. and Wakamatsu, Y. (2000). Activity of the medaka translation elongation factor 1α-A promoter examined using the GFP gene as a reporter. *Dev. Growth. Differ.* **42**, 469-478. doi:10.1046/j.1440-169x.2000.00530.x

Kinoshita, M., Murata, K., Naruse, K. and Tanaka, M. (2012). *Medaka: Biology, Management, and Experimental Protocols*. Iowa, USA: Wiley-Blackwell.

Komine, R., Nishimaki, T., Kimura, T., Oota, H., Naruse, K., Homma, N. and Fukamachi, S. (2016). Transgenic medaka that overexpress growth hormone have a skin color that does not indicate the activation or inhibition of somatolactin-α signal. *Gene* **584**, 38-46. doi:10.1016/j.gene.2016.02.046

Laiz-Carrión, R., Fuentes, J., Redruello, B., Guzmán, J. M., del Río, M. P. M., Power, D. and Mancera, J. M. (2009). Expression of pituitary prolactin, growth hormone and somatolactin is modified in response to different stressors (salinity, crowding and food-deprivation) in gilthead sea bream *Sparus auratus*. *Gen. Comp. Endocr.* **162**, 293-300. doi:10.1016/j.ygcen.2009.03.026

Leclercq, E., Taylor, J. F. and Migaud, H. (2010). Morphological skin colour changes in teleosts. *Fish. Fish.* **11**, 159-193. doi:10.1111/j.1467-2979.2009.00346.x

Lewis, V. M., Saunders, L. M., Larson, T. A., Bain, E. J., Sturiale, S. L., Gur, D., Chowdhury, S., Flynn, J. D., Allen, M. C., Deheyn, D. D. et al. (2019). Fate plasticity and reprogramming in genetically distinct populations of Danio leucophores. *Proc. Natl. Acad. Sci. USA* **116**, 11806-11811. doi:10.1073/pnas.1901021116

Lynn Lamoreux, M., Kelsh, R. N., Wakamatsu, Y. Ozato, K. (2005). Pigment pattern formation in the medaka embryo. *Pigm. Cell. Res.* **18**, 64-73. doi:10.1111/j.1600-0749.2005.00216.x

Mousa, M. A. and Mousa, S. A. (2000). Implication of somatolactin in the regulation of sexual maturation and spawning of *Mugil cephalus*. *J. Exp. Zool.* **287**, 62-73. doi:10.1002/1097-010X(20000615)287:1<62::AID-JEZ8>3.0.CO;2-0

Ota, S., Hisano, Y., Muraki, M., Hoshijima, K., Dahlem, T. J., Grunwald, D. J., Okada, Y. and Kawahara, A. (2013). Efficient identification of TALEN-mediated genome modifications using heteroduplex mobility assays. *Genes. Cells.* **18**, 450-458. doi:10.1111/gtc.12050

Pandolfi, M. B., Paz, D. A., Maggese, C., Ravaglia, M. and Vissio, P. (2001). Ontogeny of immunoreactive somatolactin, prolactin and growth hormone secretory cells in the developing pituitary gland of *Cichlasoma dimerus* (Teleostei, Perciformes). *Anat. Embryol.* **203**, 461-468. doi:10.1007/s004290100172

Pandolfi, M., Cánepa, M., Ravaglia, M., Maggese, M., Paz, D. and Vissio, P. (2003). Melanin-concentrating hormone system in the brain and skin of the cichlid fish *Cichlasoma dimerus*: anatomical localization, ontogeny and distribution in comparison to α-melanocyte-stimulating hormone-expressing cells. *Cell Tissue Res.* **311**, 61-69. doi:10.1007/s00441-002-0654-4

Pfaffl, M. W. (2001). A new mathematical model for relative quantification in real-time RT–PCR. *Nucleic Acids Res.* **29**, e45. doi:10.1093/nar/29.9.e45

Planas, J. V., Swanson, P., Rand-Weaver, M. and Dickhoff, W. W. (1992). Somatolactin stimulates in vitro gonadal steroidogenesis in coho salmon, *Oncorhynchus kisutch*. *Gen. Comp. Endocr.* **87**, 1-5. doi:10.1016/0016-6480(92)90142-7

Ramakers, C., Ruijter, J. M., Deprez, R. H. L. and Moorman, A. F. M. (2003). Assumption-free analysis of quantitative real-time polymerase chain reaction (PCR) data. *Neurosci. Lett.* **339**, 62-66. doi:10.1016/S0304-3940(02)01423-4

Ruijter, J. M., Ramakers, C., Hoogaars, W. M. H., Karlen, Y., Bakker, O., Van den Hoff, M. J. B. and Moorman, A. F. M. (2009). Amplification efficiency: linking baseline and bias in the analysis of quantitative PCR data. *Nucleic Acids Res.* **37**, e45. doi:10.1093/nar/gkp045

Sciara, A. A., Rubiolo, J. A., Somoza, G. M. and Arranz, S. E. (2006). Molecular cloning, expression and immunological characterization of pejerrey (*Odontesthes bonariensis*) growth hormone. *Comp. Biochem. Phys. C* **142**, 284-292. doi:10.1016/j.cbpc.2005.10.015

Sköld, H. N., Aspengren, S., Cheney, K. L. and Wallin, M. (2016). Fish chromatophores—from molecular motors to animal behavior. In *International Review of Cell and Molecular Biology* (ed. W. J. Kwang), pp. 171-219. San Diego, USA: Academic Press, Inc.

Stemmer, M., Thumberger, T., del Sol Keyer, M., Wittbrodt, J. and Mateo, J. L. (2015). CCTop: an intuitive, flexible and reliable CRISPR/Cas9 target prediction tool. *PLoS ONE* **10**, e0124633. doi:10.1371/journal.pone.0124633

Sugimoto, M. (2002). Morphological color changes in fish: regulation of pigment cell density and morphology. *Microsc. Res. Techniq.* **58**, 496-503. doi:10.1002/jemt.10168

Sugimoto, M., Uchida, N. and Hatayama, M. (2000). Apoptosis in skin pigment cells of the medaka, *Oryzias latipes* (Teleostei), during long-term chromatic adaptation: the role of sympathetic innervation. *Cell. Tissue. Res.* **301**, 205-216. doi:10.1007/s004410000226

Suzuki, M., Bennett, P., Levy, A. and Baker, B. I. (1997). Expression of MCH and POMC genes in rainbow trout (*Oncorhynchus mykiss*) during ontogeny and in response to early physiological challenges. *Gen. Comp. Endocr.* **107**, 341-350. doi:10.1006/gcen.1997.6936

Uchida, K., Moriyama, S., Breves, J. P., Fox, B. K., Pierce, A. L., Borski, R. J., Hirano, T. and Grau, E. G. (2009). cDNA cloning and isolation of somatolactin in Mozambique tilapia and effects of seawater acclimation, confinement stress, and fasting on its pituitary expression. *Gen. Comp. Endocr.* **161**, 162-170. doi:10.1016/j.ygcen.2008.11.031

Vargas-Chacoff, L., Astola, A., Arjona, F. J., Del Río, M. P. M., García-Cózar, F., Mancera, J. M. and Martínez-Rodríguez, G. (2009). Gene and protein expression for prolactin, growth hormone and somatolactin in *Sparus aurata*: seasonal variations. *Comp. Biochem. Phys. B* **153**, 130-135. doi:10.1016/j.cbpb.2009.02.008

Vissio, P. G., Andreone, L., Paz, D. A., Maggese, M. C., Somoza, G. M. and Strüssmann, C. A. (2002). Relation between the reproductive status and somatolactin cell activity in the pituitary of pejerrey, *Odontesthes bonariensis* (Atheriniformes). *J. Exp. Zool.* **293**, 492-499. doi:10.1002/jez.10139

Wada, H., Shimada, A., Fukamachi, S., Naruse, K. and Shima, A. (1998). Sex-linked inheritance of the lf locus in the medaka fish (*Oryzias latipes*). *Zool. Sci.* **15**, 123-126.

Zhang, Z. and Hu, J. (2006). Development and validation of endogenous reference genes for expression profiling of medaka (*Oryzias latipes*) exposed to endocrine disrupting chemicals by quantitative real-time RT-PCR. *Toxicol. Sci.* **95**, 356-368. doi:10.1093/toxsci/kfl161

Zhu, Y. and Thomas, P. (1997). Effects of somatolactin on melanosome aggregation in the melanophores of red drum (*Sciaenops ocellatus*) scales. *Gen. Comp. Endocr.* **105**, 127-133. doi:10.1006/gcen.1996.6810

Zhu, Y., Yoshiura, Y., Kikuchi, K., Aida, K. and Thomas, P. (1999). Cloning and phylogenetic relationship of red drum somatolactin cDNA and effects of light on pituitary somatolactin mRNA expression. *Gen. Comp. Endocr.* **113**, 69-79. doi:10.1006/gcen.1998.7180

Table S1

Gene	Primer sequence	Reference
ghr1	FW 5'- GAGGATGACCAAGCTTCAGAC -3' RV 5'- TGCCATGACCAAAGACCTC -3'	
ghr2	FW 5'- AGCAGGAGAATTGATGGTGG -3' RV 5'- CACCCAAGACTGACGAGAAC -3'	
rpl7	FW 5'-CGCCAGATCTTCAACGGTGTAT-3' RV 5'-AGGCTCAGCAATCCTCAGCAT-3'	Zhang and Hu *et al*. 2006

Table S1: Primer sequences used in the present study for real time PCR assays.

Figure S1

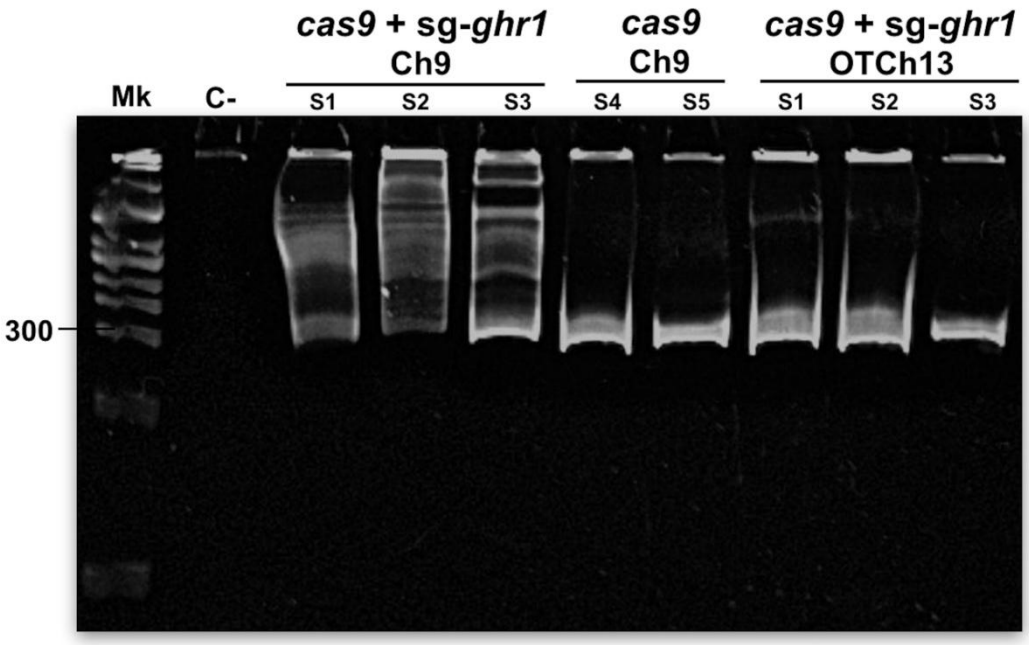

Fig. S1. Full-length gel of images of heteroduplex mobility assay (HMA). HMA to analyze to detection of off-target alterations. Representative HMA are show negative control (C-), embryos microinjected with *cas9+sg-grh1*: amplification to target gene ghr1 in chromosome 9 (ch9) samples 1,2 and 3 (S1,S2,S3), embryos microinject only with *cas9* samples 4 and 5 (S4,S5) and potential off-target loci in chromosome 13 (OTCh13) in samples 1,2 and 3.

Figure S2

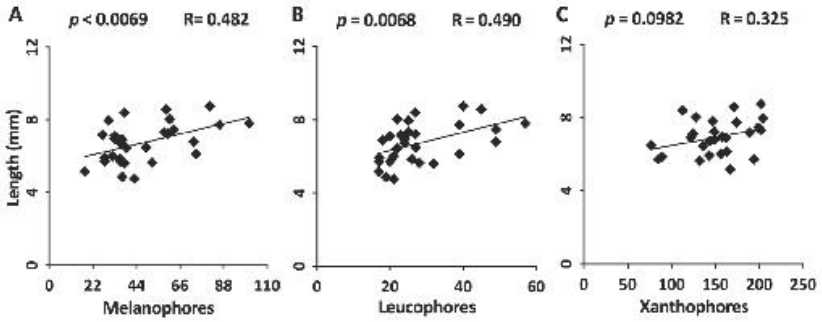

Fig. S2. Chromatophores and body length. Pearson's correlation coefficient between standard length and melanophores **(a)**, leucophores **(b)**, and xanthophores **(c).**